Semiconductors, 2024, Vol. 58, No. 6

Modified Structure of the Nanocrystalline ITO Films

© L.K. Markov[1], I.P. Smirnova[1], A.S. Pavlyuchenko[1], M.A. Yagovkina[1], V.V. Aksenova[1,2]

[1] Ioffe Institute,
194021 St. Petersburg, Russia
[2] Koltsov's Design Bureau,
198095 St. Petersburg, Russia
E-mail: l.markov@mail.ioffe.ru

Received June 18, 2024
Revised August 14, 2024
Accepted August 14, 2024

A novel method for the combined deposition of transparent conducting films of indium and tin oxide has been suggested. The method consists of sequential deposition of the material by magnetron sputtering and electron beam evaporation onto a hot substrate. The structural features and optical characteristics of the resulting films have been studied. The considered method makes it possible to modify the density of the coating, and, hence, the profile of its effective refractive index. A controlled increase in the specific surface area of films, which is achieved by the growth of nanowhiskers at the second stage of film deposition, may be in demand in a number of new devices, for example, sensors.

Keywords: indium tin oxide, ITO, nanostructured film, transparent conducting oxides, nanowhiskers.

DOI: 10.61011/SC.2024.06.59450.6796

1. Introduction

Indium tin oxide (ITO) is the most widely used of all materials providing electrical conductivity in combination with optical transparency. Thin ITO films feature an optimum combination of optical and electrical characteristics and, consequently, are used as transparent conductive contacts in a broad spectrum of devices. The tendency to form films consisting of nanowhiskers with their dimensions being significantly smaller than the radiation wavelength is an intriguing feature of ITO. Thus, under certain deposition conditions, a coating with a gradient of density and, consequently, effective refractive index in the direction perpendicular to the substrate may be formed [1]. It is known that such coatings may be antireflective due to the minimization of Fresnel reflection at their boundaries [2,3], which enables their use in fabrication of various optoelectronic elements.

The possibility of application of ITO in such devices as gas sensors [4–6] or photocatalytic devices [7,8] has been discussed more and more frequently in recent years. Since reactions in these devices proceed at the interface between the material and the environment, nanostructured films with a developed surface, which were mentioned above, may improve significantly the operational characteristics (sensitivity, speed) of such instruments.

The easiest and most technologically simple way to form coatings containing ITO filamentary crystals is their vacuum deposition via electron-beam evaporation or magnetron sputtering onto substrates preheated to high temperatures [9]. In both cases, the growth of nanowhiskers from molten In−Sn droplets proceeds by the vapor–liquid–solid (VLS) mechanism [10]. Films deposited by electron-beam evaporation contain filamentary nanocrystals with a diameter of 15−20 nm that remains virtually constant along their length, while nanocrystals of magnetron sputtered films are slightly conical: their diameter may reach 100 nm at the base and decrease to the same values of 15−20 nm at the top. Regardless of structural differences between films fabricated by these two methods, the substrate temperature in the process of deposition needs to be increased to enhance the specific surface area of films. When magnetron sputtering is used, it is also necessary to perform deposition in an oxygen-free atmosphere [11]. However, the magnitude of possible enhancement of film structuring by adjustment of the deposition conditions is limited. The number of filamentary crystals per unit surface area of a film and, consequently, the density and specific surface area of this film depend ultimately on the probability of formation of droplets of molten metal from which nanocrystals grow. In the present study, we propose to use a combined method for ITO film fabrication that involves depositing the material by magnetron sputtering at high substrate temperatures with subsequent deposition by electron-beam evaporation at the same temperatures. This provides an opportunity to alter the morphology of films to a significant extent.

2. Experimental results and discussion

Borosilicate glass slides with a thickness of 1.2 mm were used as substrates for film deposition. At the first stage, a nanostructured ITO film was formed on these glasses by magnetron sputtering. The substrates were preheated in a vacuum chamber to 550°C. An ITO target (90 wt.% In_2O_3 + 10 wt.% SnO_2) was used for deposition. High-purity (99.999%) argon served as the working gas. The films were deposited at a direct current of 200 mA ($P \sim 130$ W) and an argon pressure of 0.3 Pa. The deposition rate was

10 nm/min. The readings of a quartz thickness sensor indicated that samples with a mass content of material equivalent to a dense film 300 nm in thickness were produced. Following deposition, the chamber was filled with high-purity nitrogen to a near-atmospheric pressure (~ 80 kPa), and the sample was kept in a nitrogen atmosphere for 10 min with the heating switched on. An ITO layer with a mass content of material equivalent to a dense film 70 nm in thickness was then deposited onto the resulting film by electron-beam evaporation. High-purity (99.99%) ITO granules (90 wt.% $In_2O_3 + 10$ wt.% SnO_2) were used as the initial material for sputtering. Prior to deposition, the vacuum chamber was evacuated to a base pressure of $\sim 3 \cdot 10^{-5}$ Pa. The substrates were preheated in the vacuum chamber to 550°C, and deposition was then performed at the same temperature. The deposition rate was also 10 nm/min. As in the case of deposition by magnetron sputtering, additional annealing of the fabricated film in a nitrogen atmosphere was subsequently performed. To monitor and compare the obtained results, the material was also applied to a separate clean glass at the second stage of combined deposition in the same vacuum process.

A JSM-7001F scanning electron microscope produced by JEOL Ltd. (Japan) was used to obtain SEM images of films. X-ray diffraction measurements were carried out using a D2 Phaser (Bruker AXS, Germany) powder diffractometer. Transmittance and reflectance spectra of the samples were examined with an Optronic Laboratories OL 770 (United States) spectroradiometer. Radiation was incident onto the samples from the film side normally to the surface.

Figure 1 shows the SEM images of all films fabricated in the experiment: the magnetron sputtered film obtained at the first stage of ITO deposition (sample A); the result of ITO deposition onto a clean glass by electron-beam evaporation (sample B); and the film produced by combined deposition (sample C).

It can be seen from Figure 1 that the porous part of sample A consists of nanowhiskers with their transverse dimension decreasing from the base to the top. A significant fraction of them also form transverse branches. Since nanostructured films contain a large number of voids, the actual film thickness may be estimated at 1900 nm.

The film of sample B contains nanowhiskers with virtually equal cross sections at the top and the base. Owing to the presence of voids, the film thickness was estimated at ~ 250 nm.

The film of sample C has virtually the same thickness as the magnetron sputtered film (sample A), since the deposition of ITO by electron-beam evaporation at the second stage of the manufacturing process proceeds within the previously formed material: larger crystals of the magnetron sputtered film serve as the base for growth of small crystals of the material obtained by electron-beam evaporation, similar to how a tree trunk gives rise to small branches. Since this film contains material corresponding to a dense film with a thickness of 370 nm (300 nm at the first deposition stage + 70 nm at the second stage), the average

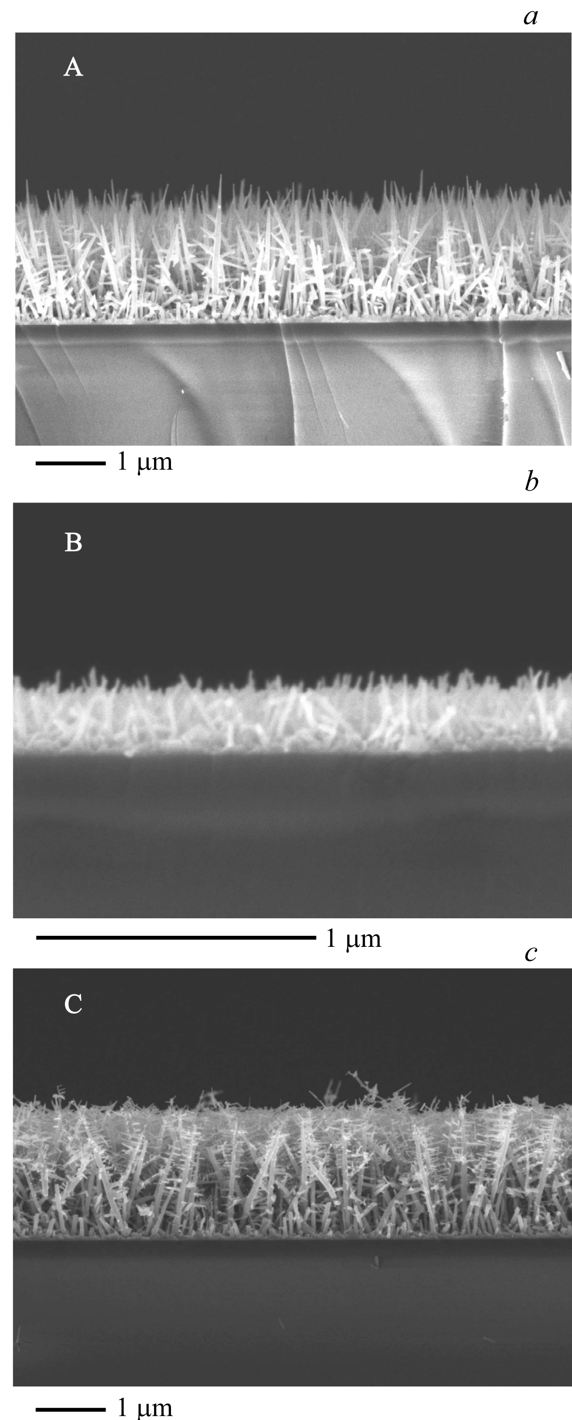

Figure 1. SEM images of cleaved surfaces of films fabricated at a temperature of 550°C by *a* — magnetron sputtering (sample A); *b* — electron-beam evaporation (sample B); *c* — combined (magnetron sputtering electron-beam evaporation) deposition (sample C).

film density increases approximately by 23%. In addition to the variation of density of the material itself, a change in the density profile of the material in the film is observed, since, as one can see from Figure 1, the material deposition at the second stage is concentrated in the upper film part due to

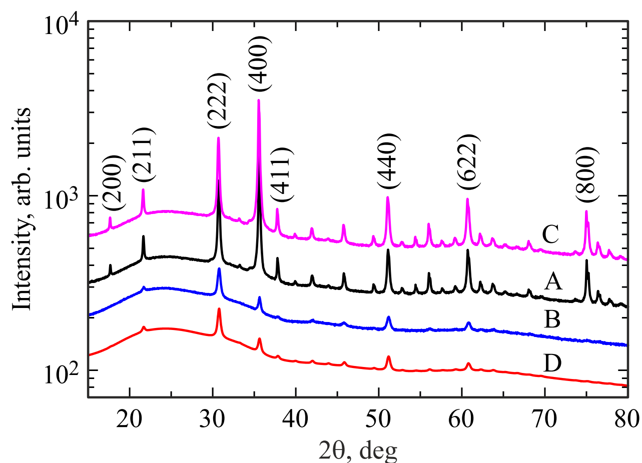

Figure 2. Diffraction curves of samples A, B, and C and calculated curve for the ITO layer on glass (D).

the fact that the film obtained at the first sputtering stage has a significant thickness.

Therefore, the effective refractive index profile of sample C differs from the one of sample A. According to the results of additional experiments that are not presented here, the voids of a thinner initial film are filled more uniformly across its thickness. Thus, one may vary both the density of resulting coatings and the distribution profile of ITO across the film thickness by adjusting the ratio of material deposited at the first and second stages of film formation.

The results of X-ray diffraction analysis revealed that the coatings consist exclusively of the material with a body-centered cubic lattice of space group $I213$ with its parameters close to cubic indium oxide In_2O_3 (PDF-2, No. 01-080-5364, $a = 10.132$ Å). Figure 2 presents the examples of diffraction curves for all samples with the Miller indices indicated for the brightest reflections. The model curve of polycrystalline ITO on a glass substrate with an average size of the coherent scattering region (CSR) of 30 nm is also shown there for comparison. The broad halo at 25° on the 2θ scale is induced by the glass substrate.

The TOPAS-5 software package (Bruker AXS, Germany) was used for analysis of structural features of the coating. A full-profile Rietveld analysis of the obtained experimental diffraction curves was carried out [12]. The average CSR size, the microstrain, and the lattice cell parameter were estimated. The results of modeling of diffraction curves are listed in the table.

The obtained results agree closely with the data from [9] where the structural features of films obtained by magnetron sputtering and electron-beam evaporation were compared. The diffraction patterns for the samples fabricated by magnetron sputtering (A) and combined deposition (C) are similar. The structure of these samples may be characterized within a model containing two phases: the first one is textureless, while the second phase is textured and has a large lattice parameter, a large crystallite size, and virtually zero microstrain. The first phase is a continuous sublayer positioned directly on the substrate, and the second phase is represented by elongated crystals seeded from this sublayer (Figure 1).

Results of modeling of diffraction curves

Samples	Average CSR size, nm	Microstrain, ε_0	Lattice parameter, Å
A	200	$0.9 \cdot 10^{-4}$	10.139
	60	$9.0 \cdot 10^{-4}$	10.134
B	30	$6.0 \cdot 10^{-4}$	10.137
C	100	–	10.140
	40	$1.2 \cdot 10^{-4}$	10.135

Sample B, which was fabricated by electron-beam evaporation, features smaller crystallites and lacks texture. This sample is characterized by a model with one component with a BCC lattice.

A comparison of the structural analysis data for films A and C (see the table) reveals that the deposition of additional material by electron-beam evaporation onto the sample prepared by magnetron sputtering leads to a reduction in the average CSR size. This statement is in good agreement with the scanning electron microscopy data (Figure 1), which, as was noted above, demonstrate the growth of small material crystals in the outer part of the film. At the same time, the average CSR size in both phases of sample C decreases compared to the CSR in sample A, indicating that small crystals that emerge at the second stage of fabrication of the combined film do not reproduce exactly the structure of larger crystals on which they grow. Apparently, this material is deposited as a third phase, but its contribution does not induce any significant change in the diffraction pattern.

The transmittance and reflectance spectra of the obtained films are shown in Figure 3. It is evident that the reflectance and transmittance of magnetron sputtered films and those produced by combined deposition are virtually indistinguishable in the long-wave region of the spectrum (red and infrared ranges), where the formation of new crystallites does not lead to detectable reflection of radiation due to the smallness of their size in comparison with the radiation wavelength. At the same time, the film produced by combined deposition reflects light more efficiently in the short-wave part of the spectrum, where the wavelength of radiation and the sizes of emerging inhomogeneities are comparable.

The experimental samples had the following values of sheet resistance: A — 54 Ω/sq; C — 38 Ω/sq. The decrease in resistance after the deposition of ITO by electron-beam evaporation may be attributed both to the deposition of a fraction of material onto the lower conductive sublayer and to the emergence of new conducting pathways due to the bridging of branches in the upper parts of the film. However, since, according to Figure 2, the dense layers of material

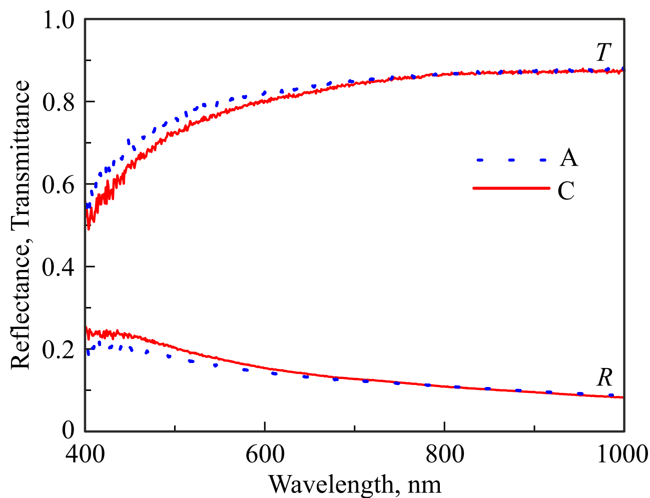

Figure 3. Transmittance (T) and reflectance (R) spectra of films obtained by magnetron sputtering (A) and combined deposition (C). (A color version of the figure is provided in the online version of the paper).

deposited directly onto the glass substrate have no visible differences in thickness or surface morphology, it is fair to assume that the primary contribution to the film resistance variation is provided by the second factor. Thus, it is highly likely that two alternative pathways for current are present in the film produced by combined deposition: the direct path along the lower dense sublayer formed at the beginning of the film fabrication and a shunting path along the percolation network consisting of nanowhiskers.

3. Conclusion

Thus, the proposed method of ITO film fabrication, which consists in two-stage deposition of the material onto preheated substrates by magnetron sputtering and electron-beam evaporation, makes it possible to vary the density and, consequently, the effective refractive index of the obtained films. The growth of a large number of thin nanocrystals at the second stage of film deposition in the considered method also allows one to enhance the specific surface area of the film material in a controlled manner. A large specific surface area may be in demand in a number of devices such as ultra-sensitive sensors.

Conflict of interest

The authors declare that they have no conflict of interest.

References

[1] L.K. Markov, A.S. Pavlyuchenko, I.P. Smirnova, S.I. Pavlov. Semiconductors, **52**, 1349 (2018).

[2] J.A. Dobrowolski, D. Poitras, P. Ma, H. Vakil, M. Acree. Appl. Optic, **41**, 3075 (2002).

[3] T. Chaikeeree, N. Mungkung, N. Kasayapanand, H. Nakajima, T. Lertvanithphol, K. Tantiwanichapan, A. Sathukarn, M. Horprathum. Optical Mater. (Amst.), **129**, 112439 (2022).

[4] Y. Zhang, Q. Li, Z. Tian, P. Hu, X. Qin, F. Yun. SN Appl. Sci., **2**, 1 (2020).

[5] A.S. Mokrushin, N.A. Fisenko, P.Y. Gorobtsov, T.L. Simonenko, O.V. Glumov, N.A. Melnikova, N.P. Simonenko, K.A. Bukunov, E.P. Simonenko, V.G. Sevastyanov, N.T. Kuznetsov. Talanta, **221**, 121455 (2021).

[6] X. Zheng, X. Qiao, F. Luo, B. Wan, C. Zhang. Sensors Actuators B: Chem., **346**, 130440 (2021).

[7] S. Kim, S.H. Kang, H.W. Choi, K.H. Kim. Mol. Cryst. Liq. Cryst., **663**, 55 (2018).

[8] J. Suo, K. Jiao, D. Fang, H. Bu, Y. Liu, F. Li, O. Ruzimuradov. Vacuum, **204**, 111338 (2022).

[9] L.K. Markov, A.S. Pavluchenko, I.P. Smirnova, V.V. Aksenova, M.A. Yagovkina, V.A. Klinkov. Thin Sol. Films, **774**, 139848 (2023).

[10] H.K. Yu, J.L. Lee. Sci. Rep., **4**, 1 (2014).

[11] V.V. Aksenova, I.P. Smirnova, L.K. Markov, A.S. Pavlyuchenko, M.A. Yagovkina. Phys. Solid State, **65**, 1995 (2023).

[12] W.A. Dollase. J. Appl. Crystallogr., **19**, 267 (1986).

Translated by D.Safin